Bridging the Multiscale gap: Identifying Cellular Parameters from Multicellular Data

Qanita Bani Baker, Gregory J. Podgorski, Christopher D. Johnson, Elizabeth Vargis, Nicholas S. Flann

***Abstract*—Multiscale models that link sub-cellular, cellular and multicellular components offer powerful insights in disease development. Such models need a realistic set of parameters to represent the physical and chemical mechanisms at the sub-cellular and cellular levels to produce high fidelity multicellular outcomes. However, determining correct values for some of the parameters is often difficult and expensive using high-throughput microfluidic approaches. This work presents an alternative approach that estimates cellular parameters from spatiotemporal data produced from bioengineered multicellular *in vitro* experiments. Specifically, we apply a search technique to an integrated cellular and multicellular model of retinal pigment epithelial (RPE) cells to estimate the binding rate and auto-regulation rate of Vascular Endothelial Growth Factor (VEGF). Understanding VEGF regulation is critical in treating age-related macular degeneration and many other diseases. The method successfully identifies realistic values for autoregulatory cellular parameters that reproduce the spatiotemporal *in vitro* experimental data.**

Key Words*—Systems Biology, Agent-Based Model, Parameter Estimation, Optimization, Micropatterning, Vascular endothelial growth factor (VEGF).

I. INTRODUCTION

An important aspect of computational systems biology is the investigation of dynamic biological processes that operate across multiple temporal and spatial scales by constructing and running multiscale models [12], [17], [9], [6], [26]. These models incorporate a set of parameters that represent the physical and chemical properties of the biological system [16]. The parameters are used to define the components of the models that when simulated reproduce the behavior of the biological system. Often the correct values of these parameters are unknown or difficult to obtain [27], [24].

Recently, there has been an increase in the number of model-fitting methods proposed to estimate model parameters' values [18], [8], [22] from experimental data. Without accurate estimations of parameters, predictions from simulation studies will most likely be erroneous and provide little scientific insight and guidance in disease treatment [2]. This scenario can be ameliorated by fitting the model to experimental *in vitro* / *in vivo* data [1] [14]. Finding the best-fit values for the unknown parameters enhances the possibility of performing accurate quantitative predictions.

Vascular endothelial growth factor (VEGF) is a key promoter of angiogenesis and vascular development and is the target in numerous anti-angiogenic therapies [5]. Angiogenesis is the growth of blood vessels from the preexisting vasculature, a process involved in the physiological functions of several diseases, such as cancer and age-related macular degeneration (AMD). Moreover, in spite of substantial basic science and translational research to develop anti-angiogenic therapies, many questions remain about the mechanisms of action of angiogenic drugs, how and why several diseases such as AMD become resistant to the treatment, or the patient conditions that can benefit most from these drugs [3]. For these reasons, computational models of angiogenesis have been developed to simulate the process and provide a framework for generating and testing hypotheses of VEGF-driven processes [11], [15], [21]. Models have aided in the development of novel and effective anti-angiogenic therapeutics that target VEGF regulation and receptors [16], [10], [28]. Advancing these computational approaches combined with progress in *in vitro* experimental studies will shed light on these issues by providing an effective framework for generating and testing hypotheses related to VEGF regulation and transport in the tissue [21].

An essential mechanism for understanding VEGF's role in disease development is its auto-regulation. The rate of VEGF secretion is controlled through an auto-inhibitory regulatory mechanism where the VEGF concentration of a cell's microenvironment down-regulates the secretion of VEGF. This control loop enables a community of cells to maintain a stable background concentration of VEGF [23]. Disruption of the loop is implicated in multiple disease states.

This paper presents a method for accurately characterizing this auto-regulation, not from microfluidic assays that interrogate individual or mixed cell populations but from spatially organized multicellular experimental data sampled over time. As will be explained later, spatiotemporal data provides unique insights because auto-regulation is inherently a mechanism that is manifested over space and time. The rest of the paper is structured as follows: First the experimental setup and computational model is described, along with the specific autoregulatory parameters that are known and those to be estimated. Second, the search method for finding the values for the parameters is described in detail. Next the method is evaluated by validating the identified parameter values. Finally, a summary of the method's effectiveness and suggestions for future work are given.

II. MULTICELLULAR EXPERIMENT AND MODEL

The experiment from which the unknown parameter values are derived employs bioengineered micropatterning techniques. The micropatterns form a regular arrangement of circular 2D patches populated with cells surrounded by an exposed substrate. The exposed regions emulate necrotic areas of the retinal tissue that result from repeated exposure to reactive oxidative species, triggering neovascularization and exudative AMD [7]. Recreating these regular spatially organized cellular configurations is essential to understanding the impact of local cell-cell and cell-environment interactions on VEGF autoregulation.

In the experimental study, described in [25], the bioengineered circular micro patterns were employed to control the extent of cell-cell interactions, which occur within the patch, and cell-environment interactions, which occur at the perimeter. Several patch sizes were used in this study ($100\,\mu\text{m}$, $200\,\mu\text{m}$, $300\,\mu\text{m}$, and $400\,\mu\text{m}$) to sample the proportion of cell-cell and cell-environment interactions in each experiment. Such sampling constrains the possible parameter values. Each patch was seeded with retinal pigment epithelial (RPE) cells and grown in a cellular culture. As the cells grew, the VEGF per cell was measured at regular intervals: 4, 24, 30 48, 54, 72 hours. To measure the VEGF per cell, enzyme-linked immunosorbent assay (ELISA) was used to determine the total VEGF contained within the cell culture, and the number of cells per patch was determined by image analysis proceeded by staining. Figure 1(a) (taken from [25]) illustrates the stained patches at 72 hours. Experiments were repeated ten times and averaged. The final spatiotemporal data produced is illustrated in Figure 1(b) and forms the target prediction for the computational model simulation.

The bioengineered experiments were simulated using a hybrid agent-based approach, which is an extension of *iDynoMiCs* framework developed by the Kreft group at University of Birmingham [13]. This model was selected because of its extensibility and easy of use. All inputs to the model such as parameter values and initial condition are easily specified using an XML document called the protocol file. Hybrid models integrate discrete components to represent the cells and continuous equations to represent biochemical reactions and diffusion. Each cell is a spherical particle that grows by consuming nutrient and accumulating biomass volume; when the volume exceeds twice the initial volume, cell division is simulated by splitting the particle into two. Particles can secrete and uptake soluble biochemicals (such as VEGF) which diffuse through the domain; regulatory reactions that model interactions among intracellular and inter-cellular proteins become PDEs. The simulation interlaces cellular growth and movement (implemented by relaxing forces between particles) with biochemical redistribution (implemented by solving the PDEs). Random noise disrupts cellular movement and the division volume to represent the inherent stochasticity of the biological processes.

The setup of the simulations replicate the experimental conditions and units of the *in vitro* experiments. The 2D domain size of each simulation is $2400\,\mu\text{m}$ by $2400\,\mu\text{m}$, initial cell size is set to $80\mu m^2$ and the doubling time due to growth is set at 36 hours. Each simulation begins with multiple RPE cells distributed randomly at the same density and with the patch pattern. The simulation replicates the first 72 hours of the *in vitro* experiments. Illustrations of the simulated experiments are shown in Figure 2.

This framework is inherently multiscale in that the parameters that control the low-level mechanisms at the cellular level, e.g., growth, the VEGF secretion rate and autoregulation, determine the cell population and VEGF concentration over the complete multicellular domain. Figure 2 illustrate the VEGF distributions in the domain. To compute the VEGF concentration per cell, the total VEGF is computed over the whole domain, while the number of cells is directly determined by the simulator. This approach intrinsically includes the quantitative

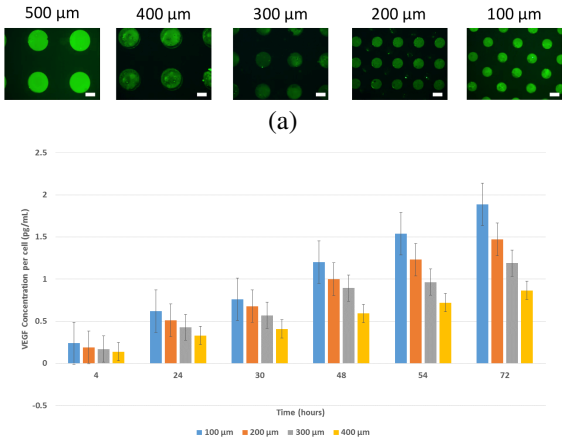

Fig. 1: (a) Patches of stained RPE cells at 72 hours for each patch size. [25]. (b) Time course of VEGF expression per cell measured at 4, 24, 30, 48, and 72 h (data for each time from the *in vitro* [25]).

spatiotemporal control effects as the cells grow, secret VEGF which diffuses over the domain. Moreover, the simulations provide insight into the spatial VEGF gradients within and between patches, unavailable in *in vitro* studies.

The autoregulation of VEGF secretion is described in Equation 1 as a function of biomass M and local VEGF concentration V. The diffusion coefficient of VEGF, D_V, is set to $5.8 \times 10^{-11} m^2 s^{-1}$ given in microfluidic experiments from [20].

$$\frac{\partial V}{\partial t} = D_V \bigtriangledown^2 V + \mu_V \frac{K}{\beta V + K} M \tag{1}$$

Over time, the RPE cells grow based on a doubling time of 36 hours [4], which determines the growth rate parameter μ_M. Since nutrient is unlimited and cell crowding is not an issue within the 72 hour time line, we applied first order kinetics for cell growth as shown in Equation 2.

$$\frac{\partial M}{\partial t} = \mu_M M \tag{2}$$

Table I summarizes the description of the parameters used in the equations above and identifies the known parameters and those that need to be determined by the method introduced in this paper.

III. METHOD

In this work, we apply a parameter fitting technique to validate a hybrid agent-based model with available *in vitro* experimental data in order to explore the best-fit values for the unknown parameters given in Table I. The three unknown parameters are termed the free parameters and together they define the vector $\bar{P} =< K, \mu_V, \beta >$. We use an error-minimization search approach that explores the space of free

TABLE I: Known and unknown parameter descriptions

Parameter	Value	Description
D_V	$5.8 \times 10^{-11} m^2 s^{-1}$	Diffusion coefficient
μ_M	1.0194 $hour^{-1}$	Max. growth rate for RPE cells
K	*Unknown*	Auto regulation rate
μ_V	*Unknown*	Secretion rate
β	*Unknown*	Binding affinity

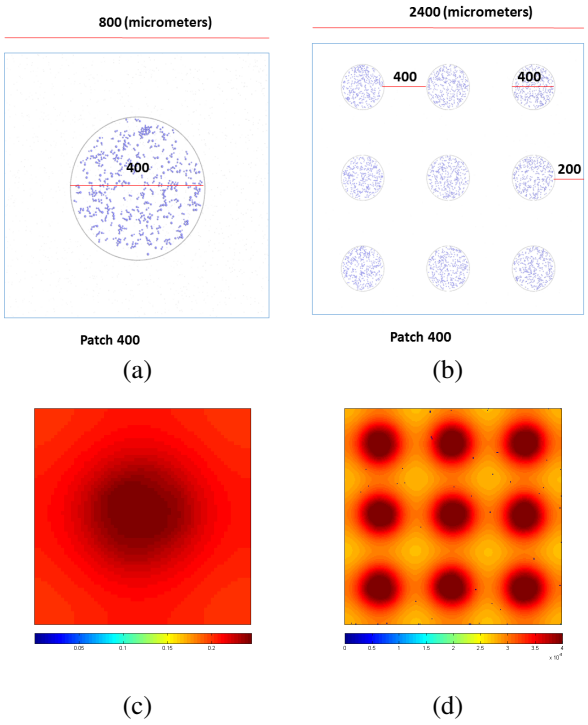

Fig. 2: (a) Closeup of initial condition of a $400\,\mu m$ patch (b) Experiment with $400\,\mu m$, 3 patches in each side. (c) Closeup of the VEGF distribution after 72 hours, (d) VEGF distribution over whole domain after 72 hours.

parameters and returns the vector $\bar{P}$ that yields the simulation results best fitting the experimental data [25]. The fitting process is summarized as follows:

Given: *Model free parameters, simulation outputs, and experimental in vitro data.*
Find: *Best-fit values for the free parameters (best $\bar{P}$)*
Such That: *The error between the simulation and experimental in vitro data is minimized.*

The search for the correct $\bar{P}$ (described in Algorithm 1 and Figure 3) starts by sweeping over an initial range of values for each free parameter being fitted. A single sweep consists of running simulations for the space of $\bar{P}$ (all combinations of free parameter values based on their ranges). The range is defined by a minimum value, a maximum value, and a step value. In a sweep, each parameter starts from its minimum value and incrementally increases to its maximum value by its step value. An error is calculated for each parameter vector by comparing the time-series outputs of the simulation with

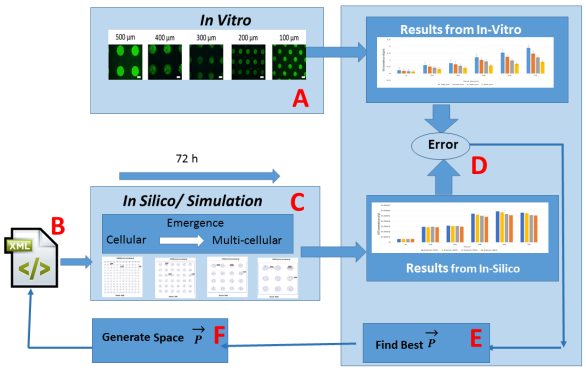

Fig. 3: An overview for the error-minimization multicellular search-based approach. In (A), RPE cells are cultured using micropatterning techniques. In (B), the parameters are initialized in the XML protocol file. In (C), a simulation is performed and the results are calculated. In (D), the error is calculated based on the difference in VEGF concentration per cell between the experimental results and simulation outputs as in Equation 3. Based on the change in error, new parameter values are selected for another simulation run (E and F). This process(B-F) will be repeated until an exit condition is met where the error improvement is below a threshold value or the search time runs out.

experimental *in vitro* data (see Figure 3D). The vector $\bar{P}$ of parameter values with the minimum error is selected and becomes the midpoint for the parameter ranges in the next sweep (see Figure 3E and F). The process continues until an exit condition is met where the reduction in error is below a threshold or the preset search time runs out. The parameter values (both free and known parameters) for a simulation are specified via the protocol file. (see Figure 3B).

In this model, the error was calculated using Equation 3. $V_s(i,t)$ and $V_e(i,t)$ are the VEGF concentrations per cell in the simulation and *in vitro*, respectively; i is the patch size, $i \in \{100, 200, 300, 400\mu m\}$ and t is the time in hours, $t \in \{4, 24, 30, 48, 54, 72 \text{ hours }\}$. The model error ($\varepsilon m$) is the sum of the errors over the four patch sizes and six time points. The error was calculated for each parameter vector $\bar{P}$. Additionally, since the simulation process is stochastic, each simulation was repeated 10 times, starting from different random seeds, and the results averaged for all presented data. Here it is important to note that this approach could be used to fit other models using different parameters, experimental results, and error functions.

$$\varepsilon m = \sum_i \sum_t (V_e(i,t) - V_s(i,t))^2 \qquad |\bar{P} =< K, \mu_V, \beta > \tag{3}$$

IV. RESULTS

Initially the method was applied to a single parameter, K. Figure 4 shows the error values for five sweep iterations over K. In each iteration, a parameter sweep for each patch size was performed. In this run, the values of VEGF secretion rate

Algorithm 1 Algorithm for the Error-Minimization Search-Based approach using parameter sweeps which identifies a parameters vector $\bar{P}$ that is locally optimal

Input: List of Free-Parameters P, XML Protocol Files P_{files}, and realistic parameter ranges Rs.
For each parameter p_k in P, initialize max_k, min_k, $step_k$ randomly within Rs.
while *time-out is not reached and* $error_{change} > error_{threshold}$ **do**
    $SWEEP(P_{files}, 1, max_1, min_1, step_1, \{\}, 10)$ ▷ Recursive parameter sweeping algorithm. Started with the first parameter. See Algorithm 2
    For each simulation result from the space of $\bar{P}$s, calculate the VEGF concentration per cell for each patch size i and time t ▷ There are 10 repeats for each simulation using different random seeds
    Calculate the $average_{VEGF}$ concentration
    Find the $error$ based on equation 3
    $error_{change}$ = $error_{previous}$ - $error$
    if $error < error_{lowest}$ **then**
        $error_{lowest} = error$ ▷ Keep track of the lowest error found so far and the change in error from the last sweep
        Change max_k, min_k, $step_k$ based on parameter values associated with $error$
    end if
end while
Return the parameters values $\bar{P}$ associated with $error_{lowest}$ ▷ this will return the best value(s) found

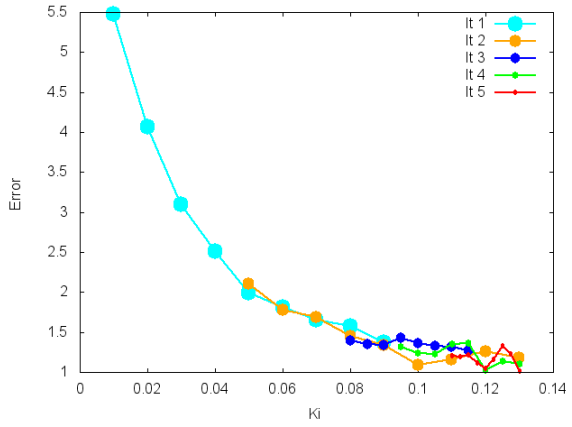

Fig. 4: Error based on different K values with iteration number It

Algorithm 2 The parameter sweep algorithm that performs a simulation for all $\bar{P}$ (a combination of free parameters). P_{files} are the XML protocol files that define the model input and initial condition, K is the parameter count, k is a counter that ranges from 1 to K, max_k is the maximum value for parameter k, min_k is the minimum value for the kth parameter, and $step_k$ is the value by which parameter k is incremented, $\bar{P}$ holds a single combination of parameter values for which a simulation will be performed, P is a matrix of size Kxj where j is the number of values in the range of some parameter (which changes as the algorithm progresses) and P[k][j] holds the jth value of the kth parameter, and Run_N is the number of repeated runs, each using different random seeds

procedure SWEEP(P_{files}, k, max_k, min_k, $step_k$, $\bar{P}$, Run_N)
    if $k = K$ **then**
        Generate XML Protocol Files G_{Pfiles} with the same setup as in P_{files} with the parameter values $\bar{P}$
        $Run(G_Pfiles, P_Set, Run_N)$ ▷ random seeds runs
        $\bar{P}.Empty$
    else
        $j = 1$
        $P[k][j] = min_k - step_k$
        while $P[k][j] < max_k$ **do**
            $P[k][j] = P[k][j] + step_k$
            $\bar{P}.Add(P[k][j])$
            $j = j + 1$
            $k = k + 1$
            $SWEEP(G_{Pfiles}, k, max_k, min_k, step_k, \bar{P}, 10)$
        end while
    end if
end procedure

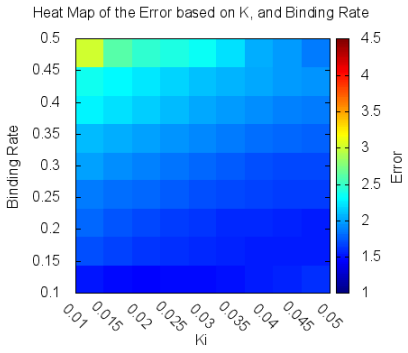

Fig. 5: The heat map of error between K and VEGF binding coefficient/rate (β) determined from the first round sweep.

μ_V and VEGF binding rate β were set to 0.09 pg/ml and 1.0, respectively. In iteration 1 ($It1$) the parameters were swept from 0.1 to 0.9, then the best value was chosen to determine the sweeping range for iteration 2 ($It2$). Over repeated sweeps the range of possible valid values for K was greatly reduced. After five iterations of sweep processes, the best K value obtained was 0.13 and the associated error was 1.01. This search considered many potential solutions and all but one were rejected as sub-optimal.

Figure 5 shows the error heat map of the first sweep iteration ($It1$) over two parameters (K and β). For this run, the VEGF secretion rate μ_V was set to 0.078 pg/ml/hour. As shown, the error is lowest when the VEGF binding rate (β) is less than 0.3 and the K value is greater than 0.03. Figure 6 shows the second sweep ($It2$), which has adjusted sweeping ranges for K and β. Successive iterations refine the parameter

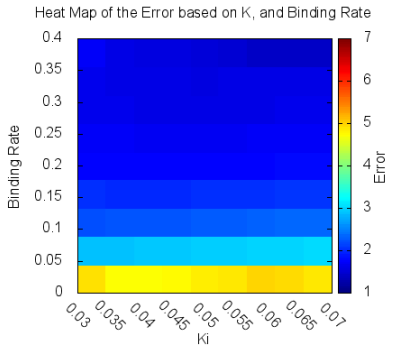

Fig. 6: The heat map of error between K and VEGF binding coefficient/rate (β) determined from the second round sweep.

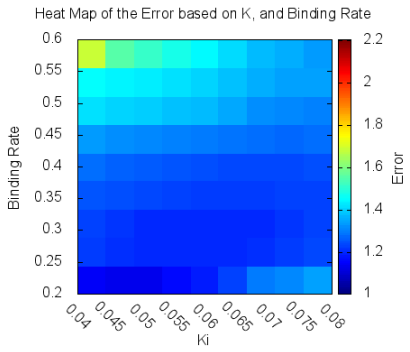

Fig. 7: The heat map of error between K and VEGF binding coefficient/rate (β) from the third round sweep.

values, as shown through reduced error in Figure 7, which shows the third sweep ($It3$). The same sweeping processes was also performed between (μ_V and K) and (μ_V and β) (data not shown).

To show how the concentration of VEGF changes over time in the simulation, VEGF expression levels were calculated at various time intervals (4, 24, 30, 48, 54, 72 h). Figure 9a shows the data from *in vitro* and Figure 9b the *in silico* model, K, μ_V, and β are set to 0.2, 0.07874 and 0.899, respectively, which were determined from a near-optimal solution discovered by the search method. The error associated with these results is 0.925. As shown in figure 9a and 9b, in both *in silico* and *in vitro*, RPE cells in the smaller patches expressed higher levels of VEGF per cell. This indicates that these cells function to maintain a consistent level of VEGF within their local microenvironment. Cells in smaller patches respond by expressing higher amounts of VEGF because the VEGF expression levels are dominated by cell-environment interactions. In contrast, larger patches maintain lower basal levels of VEGF because cell-cell auto-inhibitory regulation dominates.

Now the parameters K, μ_V and β have been determined, we replace the variables with their values in Equation 1 and set

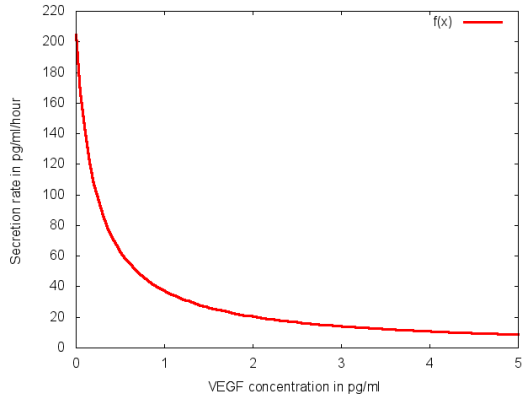

Fig. 8: The VEGF autoregulatory function of RPE cells showing how the secretion rate of VEGF is down regulated as a function of the VEGF in the microenvironment.

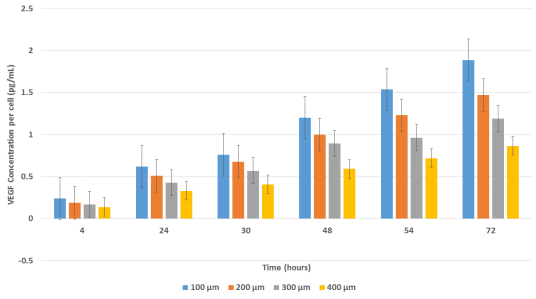

(a) Time course of VEGF expression per cell measured at 4, 24, 30, 48, and 72 h (data from the *in vitro* work [25]).

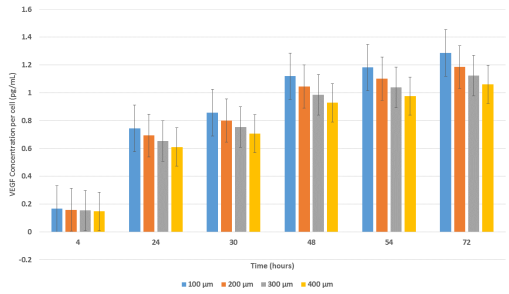

(b) Time course of VEGF expression per cell measured at 4, 24, 30, 48, and 72 h (data from the *in silico* model after optimization).

the mass M to that of a single cell ($M = 25.95pg$) resulting in the VEGF autoregulatory function for RPE cells being:

$$\frac{dV}{dt} = 0.07874 \times \frac{0.2}{0.899V + 0.2} \times 25.95 \qquad (4)$$

This function is plotted in Figure 8.

V. CONCLUSION

One of the main challenges in the computational modeling of biological systems is the determination of the models' parameters. This problem is particularly acute with multiscale

models that are gaining in popularity due to their realism. In this work, we identified the parameter values of a cellular regulatory mechanism using spatiotemporal multicellular data. While the problem of finding parameter values that describe the VEGF autoregulatory mechanism of RPE cells is simple, this problem domain serves and a proof-of-concept for the overall method. Most importantly, the method demonstrates that it is possible to utilize data at one scale to determine parameter values at a different scale.

In the work presented here, thousands of simulations were performed as the search method explored the parameter space. For each potential solution, multiple simulations were needed over each experimental case (different patch sizes) and because of the need for repeats due to model stochasticity. For the simple 2D RPE model, each simulation took less than a minute and so the process could be completed quickly. In general, the method can rapidly become infeasible as the number of unknown parameters grows, domains become larger and more complex, and the number of specific experimental cases grows.

A recently developed hybrid simulation system called Biocellion [12] could be used instead of the iDynamics to speedup the rate of simulations. Biocellion can utilize thousands of processing nodes and rapidly simulate complex models of billions of cells. The search method utilized in this paper was chosen for its simplicity and insights on the local error surfaces provided by the sweeping process. However, the fitting method is independent of the method employed to search the parameter space. Alternative methods of combinatorial optimization may improve performance.

One problem all fitting methods must deal with is under or over fitting the model. There is a possibility that the fitting problem may be under-constrained for lack of data. This problem will be explored in the RPE domain by expanding the data set to include additional studies with VEGF agonists and alternative pattern arrangements.

To extend the method to other domains, alternative error functions can be employed that measure discrepancies over a diversity of spatiotemporal features which quantify both the experimental observations and simulator outcomes. For instance, in [19] image processing is applied to bright field time-lapse images of growing yeast colonies to extract trajectories of many visual features including volume, roughness, dominant frequency etc. The same features could be extracted from the morphologies of simulated colonies and used to fit parameters of the yeast model.

ACKNOWLEDGMENT

This work was supported by the Luxembourg Centre for Systems Biomedicine, the University of Luxembourg and the Institute for Systems Biology, Seattle, USA. Research reported in this publication was partially supported by the National Institute Of General Medical Sciences of the National Institutes of Health under Award Number P50GM076547. The content is solely the responsibility of the authors and does not necessarily represent the official views of the National Institutes of Health.

REFERENCES

[1] Eva Balsa-Canto, Martin Peifer, Julio R. Banga, Jens Timmer, and Christian Fleck. Hybrid optimization method with general switching strategy for parameter estimation. *BMC Systems Biology*, 2(1):26+, March 2008.

[2] Julio R. Banga. Optimization in computational systems biology. *BMC systems biology*, 2(1):47+, May 2008.

[3] Gabriele Bergers and Douglas Hanahan. Modes of resistance to anti-angiogenic therapy. *Nature Reviews Cancer*, 8(8):592–603, August 2008.

[4] M. Bryckaert, X. Guillonneau, C. Hecquet, P. Perani, Y. Courtois, and F. Mascarelli. Regulation of proliferation-survival decisions is controlled by FGF1 secretion in retinal pigmented epithelial cells. *Oncogene*, 19(42):4917–4929, October 2000.

[5] Peter Carmeliet and Rakesh K. Jain. Angiogenesis in cancer and other diseases. *Nature*, 407(6801):249–257, September 2000.

[6] Filippo Castiglione, Francesco Pappalardo, Carlo Bianca, Giulia Russo, and Santo Motta. Modeling biology spanning different scales: an open challenge. *BioMed research international*, 2014, 2014.

[7] Amresh Chopdar, Usha Chakravarthy, and Dinesh Verma. Age related macular degeneration. *BMJ*, 326(7387):485–488, March 2003.

[8] I-Chun Chou and Eberhard O. Voit. Recent developments in parameter estimation and structure identification of biochemical and genomic systems. *Mathematical biosciences*, 219(2):57–83, June 2009.

[9] Juan G. Diaz Ochoa, Joachim Bucher, Alexandre R. Péry, José M. Zaldivar Comenges, Jens Niklas, and Klaus Mauch. A multi-scale modeling framework for individualized, spatiotemporal prediction of drug effects and toxicological risk. *Frontiers in pharmacology*, 3, 2012.

[10] Stacey D. Finley, Manjima Dhar, and Aleksander S. Popel. Compartment model predicts VEGF secretion and investigates the effects of VEGF trap in tumor-bearing mice. *Frontiers in oncology*, 3, 2013.

[11] FeilimMac Gabhann, MarianneO Stefanini, and AleksanderS Popel. Simulating Therapeutics Using Multiscale Models of the VEGF Receptor System in Cancer. In Trachette L. Jackson, editor, *Modeling Tumor Vasculature*, pages 37–53. Springer New York, 2012.

[12] Seunghwa Kang, Simon Kahan, Jason McDermott, Nicholas Flann, and Ilya Shmulevich. Biocellion: accelerating computer simulation of multicellular biological system models. *Bioinformatics*, 30(21):3101–3108, November 2014.

[13] Laurent A. Lardon, Brian V. Merkey, Sónia Martins, Andreas Dötsch, Cristian Picioreanu, Jan-Ulrich U. Kreft, and Barth F. Smets. iDynoMiCS: next-generation individual-based modelling of biofilms. *Environmental microbiology*, 13(9):2416–2434, September 2011.

[14] Gabriele Lillacci and Mustafa Khammash. Parameter Estimation and Model Selection in Computational Biology. *PLoS Comput Biol*, 6(3):e1000696+, March 2010.

[15] Feilim Mac Gabhann, James W. Ji, and Aleksander S. Popel. Computational model of vascular endothelial growth factor spatial distribution in muscle and pro-angiogenic cell therapy. *PLoS computational biology*, 2(9):e127+, September 2006.

[16] Arthur W. Mahoney, Gregory J. Podgorski, and Nicholas S. Flann. Multiobjective optimization based-approach for discovering novel cancer therapies. *IEEE/ACM transactions on computational biology and bioinformatics / IEEE, ACM*, 9(1):169–184, January 2012.

[17] Wayne Materi and David S. Wishart. Computational systems biology in drug discovery and development: methods and applications. *Drug Discovery Today*, 12(7-8):295–303, April 2007.

[18] Maria Rodriguez-Fernandez, Jose A. Egea, and Julio R. Banga. Novel metaheuristic for parameter estimation in nonlinear dynamic biological systems. *BMC bioinformatics*, 7:483+, November 2006.

[19] Pekka Ruusuvuori, Jake Lin, Adrian C. Scott, Zhihao Tan, Saija Sorsa, Aleksi Kallio, Matti Nykter, Olli Yli-Harja, Ilya Shmulevich, and Aimée M. Dudley. Quantitative analysis of colony morphology in yeast. *BioTechniques*, 56(1):18–27, January 2014.

[20] Yoojin Shin, Sewoon Han, Jessie S. Jeon, Kyoko Yamamoto, Ioannis K. Zervantonakis, Ryo Sudo, Roger D. Kamm, and Seok Chung. Microfluidic assay for simultaneous culture of multiple cell types on surfaces or within hydrogels. *Nat. Protocols*, 7(7):1247–1259, July 2012.

[21] Marianne O. Stefanini, Florence T. Wu, Feilim M. Gabhann, and Aleksander S. Popel. A compartment model of VEGF distribution in blood, healthy and diseased tissues. *BMC Systems Biology*, 2(1):77+, 2008.

[22] Jianyong Sun, J. M. Garibaldi, and C. Hodgman. Parameter Estimation Using Metaheuristics in Systems Biology: A Comprehensive Review. *Computational Biology and Bioinformatics, IEEE/ACM Transactions on*, 9(1):185–202, January 2012.

[23] Hiroyuki Takahashi and Masabumi Shibuya. The vascular endothelial growth factor (VEGF)/VEGF receptor system and its role under physiological and pathological conditions. *Clinical science (London, England : 1979)*, 109(3):227–241, September 2005.

[24] M. K. Transtrum, B. B. Machta, and J. P. Sethna. Why are nonlinear fits so challenging? *Physical Review Letters*, 104(6):060201+, December 2009.

[25] Elizabeth Vargis, Cristen B. Peterson, Jennifer L. Morrell-Falvey, Scott T. Retterer, and Charles Patrick. The effect of retinal pigment epithelial cell patch size on growth factor expression. *Biomaterials*, 35(13):3999–4004, April 2014.

[26] P. Vicini. Multiscale Modeling in Drug Discovery and Development: Future Opportunities and Present Challenges. *Clinical Pharmacology & Therapeutics*, 88(1):126–129, June 2010.

[27] Edward Walker and Chona Guiang. Challenges in Executing Large Parameter Sweep Studies Across Widely Distributed Computing Environments. In *Proceedings of the 5th IEEE Workshop on Challenges of Large Applications in Distributed Environments*, CLADE '07, pages 11–18, New York, NY, USA, 2007. ACM.

[28] Phillip Yen, Stacey D. Finley, Marianne O. Engel-Stefanini, and Aleksander S. Popel. A Two-Compartment Model of VEGF Distribution in the Mouse. *PLoS ONE*, 6(11):e27514+, November 2011.